Light-Emitting Molecular Machines: pH-Induced Intramolecular Motions in a Fluorescent Nickel(II) Scorpionate Complex

Luigi Fabbrizzi,*[a] Francesco Foti,[a] Maurizio Licchelli,[a] Paola M. Maccarini,[a] Donatella Sacchi,[a] and Michele Zema[b]

Abstract: A cyclam-like macrocycle has been synthesized with a pendant arm containing a dansylamide group. In the corresponding nickel(II) complex, binding of the pendant arm to the metal is pH controlled. In particular, at pH 4.3, the sulfonamide group deprotonates and coordinates the Ni^{II} center, giving rise to a complex of trigonal bipyramidal stereochemistry, as shown by X-ray diffraction studies performed on the crystalline complex salt. At pH 7.5, an OH^- ion binds the metal and a six-coordinate species forms. The binding-detachment of the pendant arm to/from the Ni^{II} center is signaled by changes in the emission properties of the dansyl subunit in the side chain; the fluorescence of this side chain is high when the pendant arm is not coordinated and low when the sulfonamide group is bound to the metal. The system investigated represents the prototype of a light-emitting molecular machine, driven by a pH change.

Keywords: fluorescence · macrocycles · molecular devices · nickel

Introduction

Molecular motions are observed when, in a system containing two easily distinguishable components, one component undergoes a relative displacement with respect to the other.[1] For convenience, it is assumed that one component represents the *mobile* part, and the other the *stationary* moiety. For instance, in two-station rotaxanes,[2] a wheel (the mobile part) preferentially interacts, through non-covalent and labile interactions, with one of the two stations (for example **A**, see Scheme 1 a), located along the axle (the stationary part).

If the affinity for **A** is drastically reduced by means of an external input, the wheel moves to the other station, **B**, thus giving rise to an oriented motion. On the other hand, if, following an opposite input, the affinity for **A** is re-established, the wheel moves back from **B** to **A**. In order to guarantee reversible and fast motion, the interaction of the wheel with **A** and **B** has to be non-covalent. Examples have been reported of rotaxanes where the wheel and axle are held together by π-donor–acceptor,[3] and metal–ligand interactions.[4] Similar behavior is observed if the axle is covalently closed to give a system of two interlocked rings (a 2-catenane).[2] In this case, one of the rings can undergo a half-turn rotation, following an appropriate chemical or electrochemical input.[5]

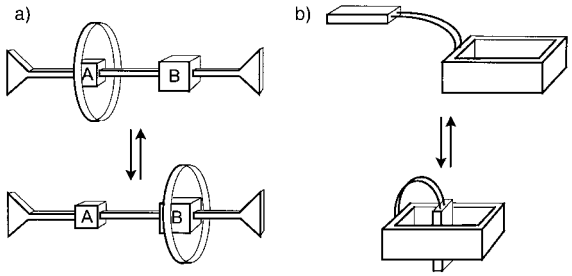

Scheme 1. Representation of the mobile and stationary parts of molecular machines. a) Wheel on an axle. b) Pendant arm permanently attaches the two parts.

Following a different approach, the mobile and stationary parts can be permanently held together by a covalent bond. This is the case illustrated in Scheme 1 b, in which a side chain (mobile component) is appended to a ring (stationary component). In particular, the pendant arm must possess some affinity for the ring cavity: if this affinity is altered (destroyed–restored through consecutive inputs of opposite nature), the arm is made to oscillate from inside the ring to outside. Again, the ring-arm interaction has to be labile, thus noncovalent. In a reported example, the side chain has at its end a π-donor group, whereas the ring is π-acceptor in nature.[6] Destruction of the donor tendencies of the appended

[a] Prof. L. Fabbrizzi, Dr. F. Foti, Prof. M. Licchelli, Dr. P. M. Maccarini, Dr. D. Sacchi
Dipartimento di Chimica Generale, Università di Pavia
via Taramelli 12, 27100 Pavia (Italy)
Fax: (+39) 0382 528544
E-mail: luigi.fabbrizzi@unipv.it

[b] Dr. M. Zema
Dipartimento di Scienze della Terra, Università di Pavia
via Ferrata 1, 27100 Pavia (Italy)

  0947-6539/02/0821-4965 $ 20.00+.50/0

group through one- or two-electron oxidation makes the side-chain dethread from the ring and move far away, in order to minimize steric repulsions.

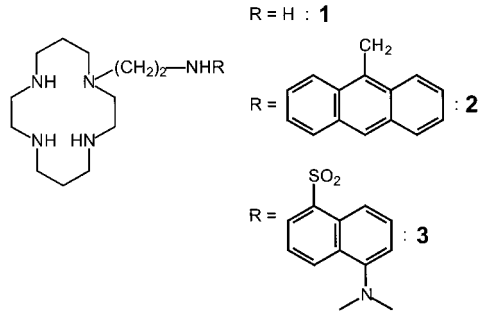

If coordinative interactions are to be considered instead, the following conditions must be met: i) a transition metal must be inserted into the ring, which is a multidentate ligand, and ii) the pendant arm must be provided with a donor atom. For instance, in the system **1**, the ring is that of the 14-membered tetramine macrocycle *cyclam*, while the pendant arm is a -$CH_2CH_2NH_2$ chain, covalently linked to a nitrogen atom of the ring.[7] Thus, the pendant arm can interact from the top with a metal (such as Ni^{II}), already encircled by the macrocycle. However, if acid is added, the apically coordinated -NH_2 group is protonated. As a consequence, the pendant arm moves away from the ring to position the ammonium group as far as possible from the ring in order to minimize the electrostatic repulsions with the metal cation. The process is illustrated in Scheme 2.

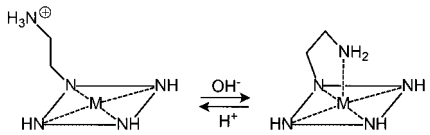

Scheme 2. System **1**: Pendant arm mechanism of interaction with the metal ion.

It should be noted that, in spite of the labile nature of the metal–amine interaction, the four amine groups of the ring do not protonate (and the metal is not extruded from the macrocycle), due to the rigidity of the ligand framework. As an example, the $[Ni^{II}(cyclam)]^{2+}$ prototype complex persists in 1M $HClO_4$ with a half-life of 30 years.[8]

Moreover, if base is added in order to neutralize the acidic solution, the ammonium group deprotonates and the amine which forms coordinates the metal center. Thus, consecutive addition of standard acid and base makes the pendant arm oscillate between two defined positions, as shown schematically in Scheme 2. Ligands like **1**, in which an aggressive tail can bite off the top of an already chelated ion (the metal), have been named *scorpionands*.[7] The first example of a scorpionand is attributed to Kaden, who investigated spectrophotometrically the stereochemical changes of the Ni^{II} complex of a ligating system in which a $-CH_2CH_2N(C_2H_5)_2$ side chain was appended to an unsaturated tetraazamacrocycle.[9] In particular, the binding detachment of the pendant arm to the metal was monitored through the pH-induced variation of the d–d spectra. More recently, in order to amplify the signal, a powerful fluorophore (anthracene) was covalently bound to an ethylamine chain linked to the cyclam framework, **2**.[10] In such circumstances, the binding detachment of the pendant arm to/from the metal was signaled by the switching on/off of the fluorescent emission. In particular, at $pH < 3$, the side chain was in the ammonium form and was located far away from the metal (fluorescence on). At $pH > 3$, the pendant arm was in the amine form and was coordinated to the metal (fluorescence off). Thus, consecutive addition of standard acid and base, to make pH lower/higher than 3, turned fluorescence on/off, providing an example of mechanically operated molecular switch of fluorescence.

Here, we describe a new example of a fluorescent scorpionand, **3**, in which the pendant arm contains a secondary sulfonamide group belonging to the dansyl fluorophore. The sulfonamide group itself does not display coordinating properties and is a very weak acid in aqueous solution. However, in the presence of divalent late transition metal ions, it can deprotonate and coordinate the metal. This event is expected to take place at a relatively high pH, certainly higher than 3. The deprotonation of aromatic sulfonamides promoted by coordination to a metal ion has been reported in the past.[11] For instance, Kimura described the behavior of macrocyclic ligands bearing a tosylamide or a dansylamide moiety on a side arm: at neutral pH, they form zinc(II) complexes in which the deprotonated nitrogen of the sulfonamide is bound to the metal ion.[11a,b]

Very interestingly, the Ni^{II} complex of **3** with the deprotonated sulphonamide group was isolated in the crystalline form and its molecular structure was determined. This is the first reported structure of a nickel(II) scorpionate complex in which the nitrogen atom of the pendant arm is coordinated to the metal, and discloses some unexpected geometrical features. In particular, it shows a distorted trigonal bipyramidal arrangement of the five amine nitrogen atoms.

Results and Discussion

Synthesis of scorpionand 3: The dansyl-tetraazamacrocycle conjugate **3** was prepared according to a three-step synthesis (see Scheme 3) involving i) triprotection of cyclam, ii) functionalization of the macrocyclic framework and iii) deprotection.

The protection of three secondary amino groups of cyclam by *tert*-butoxycarbonyl (Boc) groups, which was carried out by a modified literature method,[12] was performed in order to obtain the mono-functionalized macrocyclic ligand with satisfactory purity. Any attempt to obtain the dansylderivative **3** by direct reaction of unprotected cyclam (five-fold excess) with dansylaziridine afforded mixtures of the mono- and disubstituted products which could not be efficiently separated by common chromathographic methods. The final deprotection step, carried out in trifluoroacetic acid, afforded compound **3** with an overall yield of about 38% (referred to cyclam).

0947-6539/02/0821-4966 $ 20.00+.50/0 *Chem. Eur. J.* **2002**, *8*, No. 21

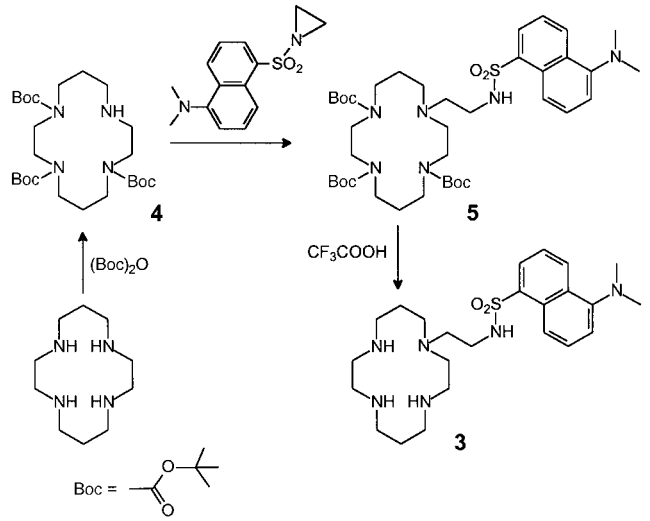

Scheme 3. Preparation of dansyltetraazamacrocycle **3**.

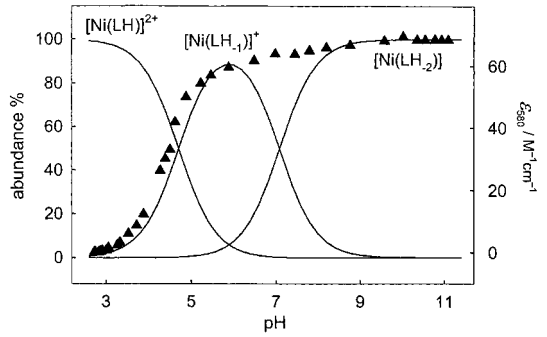

Figure 1. Left vertical axis, distribution curves of the species present at equilibrium for the Ni^{II} complex of scorpionand **3** in $EtOH/H_2O$ 4:1 (*v*/*v*) solution at 25° C. Right vertical axis (▲), molar absorbance measured at 580 nm.

Acid–base equilibria involving the Ni^{II} scorpionate complex: The acid–base properties of the Ni^{II} complex of scorpionand **3** were investigated through titration experiments. In particular, a solution of $[Ni^{II}(\mathbf{3})](ClO_4)_2$ in $EtOH/H_2O$ 4:1, for which the pH had been adjusted to 2.5 with perchloric acid, was titrated with standard sodium hydroxide. Non-linear least-squares fitting of the titration curve (pH vs. equivalents of NaOH) showed that the investigated complex behaves as a diprotic acid, with $pK_{A1} = 4.30 \pm 0.08$ and $pK_{A2} = 7.49 \pm 0.04$ (at 25 °C, ionic strength adjusted to 0.1 M with $NaClO_4$). Thus, for LH indicating the amide scorpionand **3**, the following three species are present in solution, moving from pH 2.5 upwards: $[Ni^{II}(LH)]^{2+}$, $[Ni^{II}(LH_{-1})]^{+}$, $[Ni^{II}(LH_{-2})]$. The $-n$ subscript notation indicates that n hydrogen ions have been released from the complex: accordingly, the $[Ni^{II}(LH_{-1})]^{+}$ species has lost one proton, while the $Ni^{II}(LH_{-2})]$ neutral complex has lost two.

The variation of the percent abundance of the three species at equilibrium with increasing pH is plotted in the distribution diagram shown in Figure 1. It may be seen that the doubly positively-charged complex $[Ni^{II}(LH)]^{2+}$ is present at 100 % for pH ≤ 3, the neutral species $[Ni^{II}(LH_{-2})]$ is present at 100 % at pH ≥ 9, whereas the intermediate monopositive complex $[Ni^{II}(LH_{-1})]^{+}$ reaches its maximum concentration (90 %) at pH 6.

$[Ni^{II}(LH)]^{2+}$ complex: The solution at pH ≤ 3, which contains 100 % of the $[Ni^{II}(LH)]^{2+}$ complex, exhibits a pale yellow color. The color is a result of the tail in the visible region of the absorption band of the dansyl chromophore, centered at $\lambda_{max} = 334$ nm (molar absorbance $\varepsilon = 4150\ M^{-1}cm^{-1}$). The spectrum also shows very weak d–d bands at 572 nm ($\varepsilon = 6\ M^{-1}cm^{-1}$) and 965 nm ($8\ M^{-1}cm^{-1}$). The latter spectral features are typical of an octahedral high-spin Ni^{II} complex (the highest energy d–d band, expected in the 340–350 nm range, is obscured by the dansylamide band).[13] In the $[Ni^{II}(LH)]^{2+}$ complex, the pendant arm is in the sulphonamide form and, since the amide nitrogen atom does not possess any coordinating tendency, the side chain is expected to point outwards from the ring. Under these circumstances, the Ni^{II} ion should be chelated in a coplanar fashion by the tetramine ring, a geometrical situation typically observed with nickel(II) complexes of cyclam. Moreover, two solvent molecules (such as H_2O) should occupy the two axial positions of the elongated octahedron, to complete the six-coordination. The hypothesized structure of the $[Ni^{II}(LH)]^{2+}$ complex is pictorially sketched in Scheme 4a.

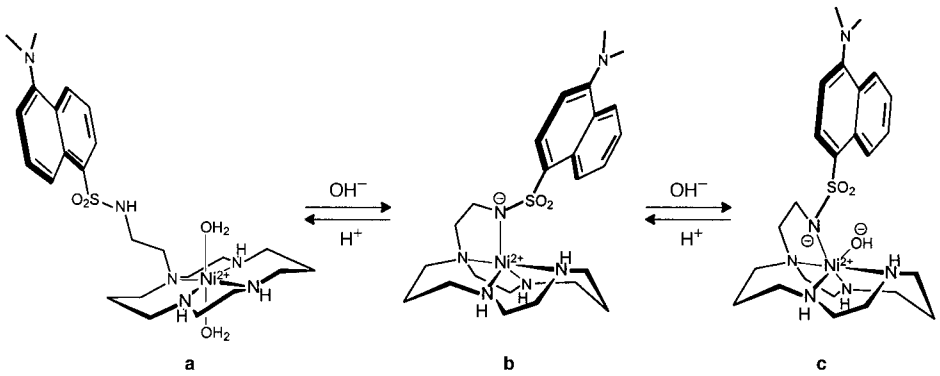

Scheme 4. Complexes $[Ni^{II}(LH)]^{2+}$, $[Ni^{II}(LH_{-1})]^{+}$ and $[Ni^{II}(LH_{-1})(OH)]$.

No band is observed at 450 nm, where low-spin Ni^{II} tetramine complexes of square-planar geometry typically absorb.[13] Thus, the presence of a high-spin (octahedral)/low-spin (square planar) equilibrium mixture, which is observed with the reference complex $[Ni^{II}(cyclam)]^{2+}$, has to be ruled out.

$[Ni^{II}(LH_{-1})]^{+}$ complex: In the course of the titration, it was observed that the pale yellow solution, on increasing pH, took on a rather intense blue color. Spectrophotometric investigation showed that the appearance of the blue color corresponded to the development of a spectrum whose major band was centered at $\lambda_{max} = 582$ nm, with a molar absorbance $\varepsilon = 67\ M^{-1}cm^{-1}$. The variation with pH of the absorbance of such a

band is superimposed on the distribution diagram displayed in Figure 1. It is observed that the absorbance (black triangles) begins to increase at pH 3 and superimposes well on the ascending arm of the concentration profile of $[Ni^{II}(LH_{-1})]^+$. Thus, the development of the d–d absorption band at 582 nm (and appearance of the blue color) corresponds to the formation of the $[Ni^{II}(LH_{-1})]^+$ complex. In particular, the absorbance reaches a limiting value at around pH 6, corresponding to highest concentration of the $[Ni^{II}(LH_{-1})]^+$ complex. Variations of the d–d spectra of transition metal complexes are typically associated with geometrical changes. The observed spectral features suggest that the deprotonation process involves the sulphonamide group and that, following the simultaneous folding of the pendant arm, the deprotonated nitrogen atom goes on to coordinate the Ni^{II} center. This hypothesis is also supported by spectral changes in the 300–350 nm interval, where the intramolecular charge-transfer transition of the dansylamide fragment is typically observed. In particular, when moving from pH 2.5 ($[Ni^{II}(LH)]^{2+}$ complex) to pH 6 ($[Ni^{II}(LH_{-1})]^+$ complex), the charge-transfer band moves from 334 to 312 nm and becomes distinctly more intense (ε increases from 4150 to 6450 $M^{-1}cm^{-1}$).

These drastic variations (see spectra in Figure 2) are consistent with sulphonamide deprotonation, an event that significantly alters the charge distribution in the dansylamide moiety, thus modifying energy and feasibility of the charge-transfer transition.

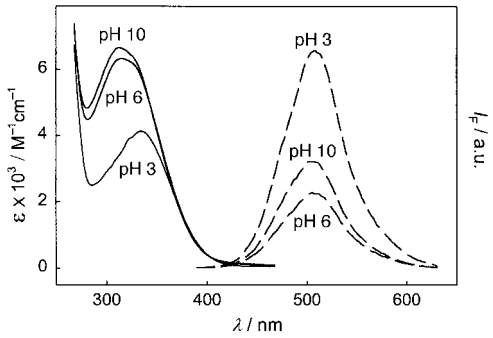

Figure 2. Absorption (solid lines) and emission spectra (dashed) of $[Ni^{II}(\mathbf{3})]ClO_4$ dissolved in EtOH/H_2O 4:1 (*v*/*v*) at different pH. Numbers close to each spectrum indicate the corresponding pH values.

Most interestingly, slow diffusion of diethyl ether into an ethanol/water solution (4:1, *v*/*v*, adjusted to pH 7) of the complex afforded blue crystals of a salt of formula $[Ni^{II}(LH_{-1})]ClO_4$, suitable for X-ray diffraction studies. The crystal structure consists of one $[Ni^{II}(LH_{-1})]^+$ molecular cation, one perchlorate anion and one water molecule, which do not interact with the metal center. The Ortep plot of the complex $[Ni^{II}(LH_{-1})]^+$ is shown in Figure 3.

Two important features are evident: i) the nitrogen atom of the deprotonated sulphonamide group is coordinated to the metal; ii) the metal center is not chelated in a coplanar manner by the macrocycle, but is coordinated according to a rather distorted trigonal bipyramidal geometry. In particular, the two axial sites of the distorted trigonal bipyramid are

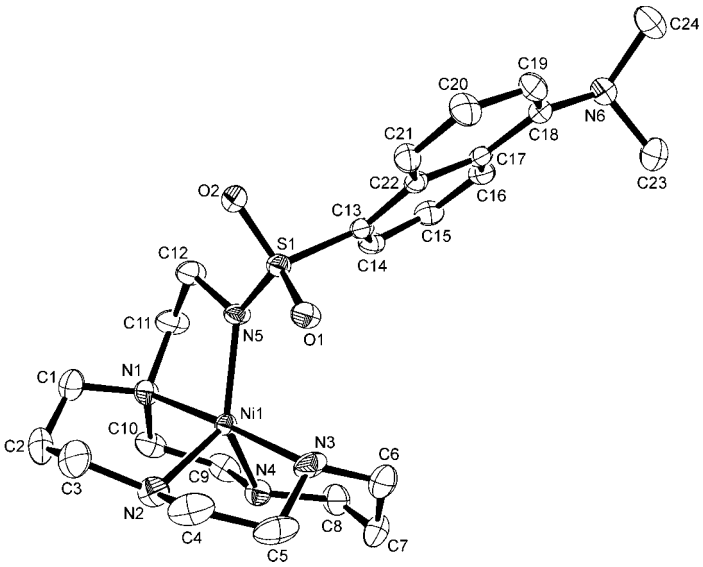

Figure 3. Ortep view of $[Ni^{II}(LH_{-1})]ClO_4$ with thermal ellipsoids drawn at 20% probability level. Perchlorate anions were omitted for clarity. Selected bond lengths: Ni1–N1 2.112(3), Ni1–N2 2.047(4), Ni1–N3 2.085(4), Ni1–N4 2.057(4), Ni1–N5 2.008(3). Selected bond angles: N1-Ni1-N2 94.26(17), N1-Ni1-N3 175.69(16), N1-Ni1-N4 84.83(16), N1-Ni1-N5 82.89(14), N2-Ni1-N3 84.97(19), N2-Ni1-N4 103.14(16), N2-Ni1-N5 124.21(17), N3-Ni1-N4 91.20(17), N3-Ni1-N5 101.07(15), N4-Ni1-N5 131.70(16).

occupied by two non-consecutive nitrogen atoms of the macrocycle: N1, to which the pendant arm is linked, and N3. Notice that the N1-Ni^{II}-N3 angle is 176.2°, only slightly lower than the regular value of 180°. On the other hand, the atoms N2, N4 and N5 occupy the three equatorial sites of the trigonal bipyramid [Ni1 is 0.113(1) Å out of the N2–N4–N5 mean-plane], even if the angles between the equatorial bonds deviate substantially from the normal value of 120°: in particular, N5-Ni^{II}-N2 124.5°, N5-Ni^{II}-N4 132.2°, N2-Ni^{II}-N4 102.3°. The Ni^{II}–N bond lengths involving the amine groups of the macrocycle range from 2.05 to 2.11 Å, which are the values expected for a Ni^{II} (high-spin)–sp^3 nitrogen atom. On the other hand, the bond to the deprotonated sulphonamide is remarkably short, 2.01 Å. This may be due to the fact that this nitrogen atom is planar and is sp^2 hybridized [in fact, the Ni1-N5-S1-C12 group is almost planar, as revealed by a calculation of the best plane using all the four atoms. The mean deviation is 0.032 Å, while the maximum deviation is 0.074(4) Å for N5]. Thus, the release of one hydrogen ion from the sulphonamide group, which takes place at pH = pK_{A1} = 4.30, induces a drastic geometrical change. The side chain folds on the macrocyclic ring and the deprotonated sulphonamide group binds the metal center (see structural sketches **a** and **b** in Scheme 4). At the same time, in order to favor the interaction with the deprotonated amide nitrogen atom, the metal moves out of the plane of the four macrocyclic donor atoms and expels the two water molecules, while the five nitrogen atoms rearrange to give a distorted trigonal bipyramidal coordination geometry. This geometrical rearrangement accounts for the spectral changes and appearance of a relatively intense blue color occurring at pH 4.30. In fact, the starting complex, the trans-octahedral $[Ni^{II}(LH)$

0947-6539/02/0821-4968 $ 20.00+.50/0 *Chem. Eur. J.* **2002**, *8*, No. 21

$(H_2O)_2]^{2+}$, is centrosymmetric and its d–d transitions are intrinsically Laporte forbidden. This explains the very low intensity of the absorption bands ($\varepsilon = 1-5\,M^{-1}cm^{-1}$). On deprotonation, the complex rearranges to the trigonal bipyramidal stereochemistry with all the nitrogen atoms coordinated. On changing from an octahedron to a trigonal bipyramid, the center of symmetry is lost and d–d transitions become Laporte allowed. This explains the higher intensity of absorption bands in the visible region and appearance of a relatively intense color.

$[Ni^{II}(LH_{-2})]$ complex: As the concentration of $[Ni^{II}(LH_{-1})]^+$ decreases and the complex $[Ni^{II}(LH_{-2})]$ begins to form, following an increase in pH, the intensity of the band at 580 nm (filled triangles in Figure 1) increases very slightly and reaches a plateau with the formation of 100% of the neutral complex. The second deprotonation process, occurring at $pH = pK_{A2} = 7.5$, cannot involve any of the amine nitrogen atoms of the macrocycle. It is therefore suggested that it is a water molecule that deprotonates and the OH^- ion which forms goes to bind the Ni^{II} center, giving rise to a neutral six-coordinate complex. Thus, the formula of the $[Ni^{II}(LH_{-2})]$ species should be more accurately written: $[Ni^{II}(LH_{-1})(OH)]$. In the absence of X-ray diffraction data, it is not possible to say whether six-coordination corresponds to the formation of a regular octahedron (with the Ni^{II} ion chelated in a coplanar fashion by the tetramine macrocycle) or to a distorded arrangement in which, for instance, the OH^- ion has approached the metal in the middle of Ni^{II}–N4 and Ni^{II}–N5 bonds, which form a rather large angle (132.2°). A tentative structural sketch of the $[Ni^{II}(LH_{-1})(OH)]$ complex, which refers to the distorted octahedral stereochemistry, is pictorially illustrated in Scheme 3c. It is of note that the geometrical rearrangement, when moving from $[Ni^{II}(LH_{-1})]^+$ to $[Ni^{II}(LH_{-1})(OH)]$, does not alter the d–d spectrum, which simply increases in intensity, reaching a limiting value at pH 9. Also the charge-transfer band does not change substantially, when moving from pH 6 to 10 (see spectra in Figure 2). In particular, λ_{max} remains the same and the molar absorbance increases slightly (from 6450 to $6850\,M^{-1}cm^{-1}$). In fact, binding of a hydroxide ion to the metal center is not expected to significantly alter the nature of the dipole located in the deprotonated dansylamide fragment and responsible for the intramolecular charge transfer transition.

If standard acid is added to the basic solution, the intensity of the band at 580 nm progressively decreases and the blue color vanishes. In particular, the absorbance profile measured with decreasing pH superimposes well on the profile measured with increasing pH (filled triangles in Figure 1). This demonstrates that the stereochemical rearrangements accompanying the two acid-base steps are fast, reversible and kinetically uncomplicated.

Motion of the pendant arm signaled by light emission: The acid–base behavior of the Ni^{II} complex of **3**, which involves the swinging of the pendant arm (**a** → **b** in Scheme 4), could also be followed by looking at the emission features of the dansyl fluorogenic fragment. In fact, the dansyl group, when irradiated at 332 nm (absorption of the charge-transfer complex), shows a rather broad and unstructured emission band with $\lambda_{max} = 510$ nm (see Figure 2). Such an emission band is present in the fluorescence spectrum of an acidic solution of the Ni^{II} complex of **3**, that is a solution of the $[Ni^{II}(LH)(H_2O)_2]^{2+}$ species.

The intensity of the emission band at $\lambda_{max} = 510$ nm, I_F, is plotted against pH in Figure 4 (filled triangles), in a diagram which reports also the percentage abundance of the three complexes present at the equilibrium: $[Ni^{II}(LH)(H_2O)_2]^{2+}$, $[Ni^{II}(LH_{-1})]^+$, and $[Ni^{II}(LH_{-1})(OH)]$. It is observed that, in the pH interval 2.5–3.5, I_F keeps its maximum value. Then, on raising the pH, as the concentration of $[Ni^{II}(LH)(H_2O)_2]^{2+}$ decreases and that of $[Ni^{II}(LH_{-1})]^+$ increases, I_F diminishes, to reach its minimum value at pH 6, coinciding with the highest concentration of $[Ni^{II}(LH_{-1})]^+$. On further increasing the pH, with the decrease of the concentration of $[Ni^{II}(LH_{-1})]^+$ and the increase of the concentration of $[Ni^{II}(LH_{-1})(OH)]$, I_F grows again to reach a plateau at a higher pH, when the $[Ni^{II}(LH_{-1})(OH)]$ species is formed at 100%. This limiting value corresponds at about 50% of the original fluorescence intensity. Summing up, we observe full emission of the dansyl fragment in the complex $[Ni^{II}(LH)(H_2O)_2]^{2+}$ (structure **a** in Scheme 4); then, fluorescence is quenched substantially in the complex $[Ni^{II}(LH_{-1})]^+$ (**b**); finally, dansyl emission is partially restored in the complex $[Ni^{II}(LH_{-1})(OH)]$ (**c**).

Such behavior has to be related to different effects exerted by the metal center on the fluorogenic fragment. In $[Ni^{II}(LH)(H_2O)_2]^{2+}$ (**a**), the dansyl subunit is far away from the metal and there is no way of establishing through-bond interactions between the Ni^{II} center and the fluorophore, especially in view of the presence in the chain of an insulating $-CH_2CH_2-$ spacer. On the other hand, in $[Ni^{II}(LH_{-1})]^+$ (**b**), the Ni^{II} center can communicate with the aromatic subunit through the coordinative bond and the $-NS(O_2)-$ group and can quench the excited fluorophore through either an electron transfer (eT) or an electronic energy transfer (ET) process. Such a communication effect is partially reduced in $[Ni^{II}(LH_{-1})(OH)]$ (**c**), when the coordination geometry rearranges from trigonal bipyramidal to (distorted) octahedral and the coordination number changes from 5 to 6. The emissive response was found to be quickly reversible, as, on back titration from pH 11.5 to 2.5, an I_F profile was obtained, which was perfectly superimposable on the profile obtained in the direct titration. This is shown in Figure 4 (filled triangles).

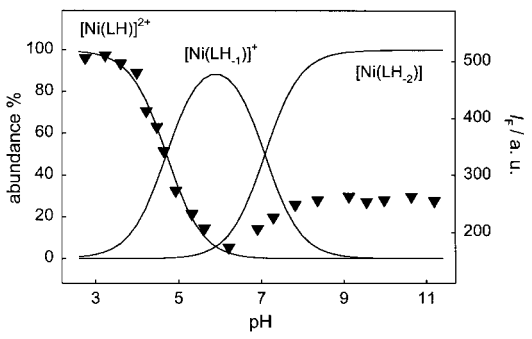

Figure 4. Left vertical axis, distribution curves of the species present at equilibrium for the Ni^{II} complex of scorpionand **3** in $EtOH/H_2O$ 4:1 solution at 25°C. Right vertical axis (full triangles), fluorescence intensity measured at 510 nm.

  0947-6539/02/0821-4969 $ 20.00+.50/0

In regard to the quenching process taking place in the complex $[Ni^{II}(LH_{-1})]^+$, we are inclined to believe that it has to be ascribed to an ET mechanism (Dexter type). We measured emission spectra on an EtOH solution of $[Ni(LH_{-1})]ClO_4$, both at room temperature and at 77 K (glassy matrix) and we observed that freezing of the solution at liquid nitrogen temperature did not cause any fluorescence revival. This behavior would suggest that an ET process is active.[14] Exceptions refer to sufficiently exoergonic and ultra-fast eT processes, which take place both at room temperature and in a glassified matrix.[15] It should also be considered that the occurrence of an eT process in the $[Ni^{II}(LH_{-1})]^+$ complex is unfavored from a thermodynamic point of view. In particular, the free energy change associated with the Ni^{II}-to-excited fluorophore eT process ($Dns^* + Ni^{II} \rightarrow Dns^- + Ni^{III}$) is distinctly positive: $\Delta G^0_{eT} \geq 1.3$ eV. Such a quantity can be estimated through the appropriate combination of photophysical and electrochemical data: $E^{0-0}(Dns) = 2.4$ eV; $E^0(Ni^{III}/Ni^{II}) = 0.70$ V versus Fc^+/Fc in MeCN; $E^0(Dns/Dns^-) \leq -3.0$ V versus Fc^+/Fc in MeCN.[16]

Conclusion

The aim of this work was the design of a metal scorpionate complex, in which the movement of the tail could be controlled from outside and signaled through a change in the light emission. We have observed that the Ni^{II} complex of the functionalized macrocycle **3** does this job well, as the sulphonamide group present in the pendant arm deprotonates and the arm folds to coordinate the metal in a slightly acidic solution. The process is fast and reversible and can be repeated in principle indefinitely, without any fatigue, by varying the pH back and forth between 2 and 6. Swinging of the pendant arm can be monitored by a color change and, most efficiently, by quenching-revival of the emission of a fluorogenic fragment which had been appended to the side-chain. In particular, fluorescence is high when the pendant arm is not coordinated and the fluorophore remains far away from the metal center. Fluorescence is low when the side chain is coordinated to the metal, which can communicate electronically with the photo-excited fluorophore. A second acid/base event takes place at higher pH, but this does not involve the pendant arm, which remains coordinated to the metal.

Multicomponent systems able to undergo controllable motions convert (chemical) energy into mechanical work in a repeatable way and are therefore considered *molecular machines*. Rotaxanes and catenanes were the first deliberately designed machines, operating at the molecular level. Metal scorpionates, like the Ni^{II} complexes of **2** and **3**, constitute a second class of machines, where the activity is accompanied by variations of light emission. In analogy to the machines of the macroscopic world, $[Ni^{II}(\mathbf{2})]^{2+}$ and $[Ni^{II}(\mathbf{3})]^{2+}$ are constituted by fixed and interchangeable components. For instance, the cyclam-like tetramine ring is a common piece, and is required to keep the metal in place, even in strongly acidic conditions. The pendant arm must contain both an acid/base site and a light-emitting fragment. In system **2**, the acid is an ammonium group, with pK_A 3. Thus, the dangling motion of the side chain takes place in rather acidic conditions. In system **3**, the acid (a sulphonamide group) is distinctly weaker, so that deprotonation and concurring intramolecular motion take place in a solution closer to neutrality. Another component that can be replaced is the luminescent subunit. In the systems being considered here, **2** possesses an anthracene fragment, which emits UV light, whereas the dansylamide subunit of **3** fluoresces in the full visible region. This work has demonstrated that an appropriate choice of the components of the pendant arm allows tuning of the behavior of light-emitting molecular machines.

Experimental Section

General remarks: Unless otherwise stated, commercially available reagent grade chemicals (Sigma-Aldrich) were used as received. 1,4,8,11-Tetraazacyclotetradecane (cyclam) was prepared according to the literature method.[17] Column chromatography was carried out on silica gel 60 (Merck 9385). Spectrophotometric or fluorimetric grade solvents were used for spectroscopic measurements.

UV/Vis spectra were recorded on a Hewlett–Packard 8452A diode array spectrophotometer; emission spectra were recorded on a Perkin–Elmer LS-50B luminescence spectrometer. Emission spectra at 77 K were measured in ethanol (10^{-5} M), using quartz sample tubes and the same luminescence spectrometer equipped with a Perkin–Elmer low-temperature luminescence accessory.

NMR spectra were recorded on a Bruker AMX400 spectrometer. Mass spectra were obtained using an LCQ DECA ion-trap mass spectrometer equipped with electrospray ionization (ESI) ion source and controlled by Xcalibur software 1.1 (Thermo-Finnigan).

Potentiometric determinations were performed in a thermostated cell on ethanol/water (4:1 *v*/*v*) solutions (25 mL, made to 0.1 M in $NaClO_4$, 25 °C) containing $[Ni^{II}(LH_{-1})]ClO_4$ (8.5×10^{-4} M) and an excess of standard $HClO_4$, by addition of standard aqueous NaOH (a Radiometer automatic titration apparatus was used). The pH scale was calibrated prior to each experiment according to the Gran method.[18] Refinement of the potentiometric data was made through the Hyperquad package.[19]

Spectrophotometric and spectrofluorimetric titrations were performed on ethanol/water (4:1 *v*/*v*) solutions (25 mL, made to 0.1 M in $NaClO_4$, 25 °C) of $[Ni^{II}(LH_{-1})]ClO_4$ (10^{-3}–10^{-5} M) adjusted at pH ≈ 2.5 by adding small amounts of a standard solution of $HClO_4$. Additions of standard solutions of 0.1 M NaOH were then made until a basic pH (≈11.5) was obtained. Absorption or emission spectra ($\lambda_{exc} = 368$ nm) were taken after each addition of base. Excitation was performed at 368 nm as absorbance undergoes only negligible variations at this wavelength in the course of the titration experiment.

Safety note: Perchlorate salts of metal complexes are potentially explosive and should be handled with care. In particular, they should never be heated as solids.[20]

1,4,8-Tris(*tert*-butoxycarbonyl)-1,4,8,11-tetraazacyclotetradecane (4): Cyclam (1.0 g, 5 mmol) was dissolved in dried dichloromethane (200 mL) and triethylamine was added (25 mmol) under a dinitrogen atmosphere. The reaction mixture was stirred and a solution of di-*tert*-butyl-dicarbonate (1.96 g, 9 mmol) in dried dichloromethane (60 mL) was added dropwise. After cooling the reaction mixture to −15 °C, another portion of *tert*-butoxy-dicarbonate (6 mmol) was added, and the mixture was stirred at room temperature overnight. The solution was treated with 0.5 N Na_2CO_3 and the organic solution dried over Na_2SO_4. The solvent and the excess of triethylamine were removed in vacuo and the residue was purified by liquid chromatography (silica gel, ethyl acetate/methanol 9:1, $R_f = 0.5$); yield 70.5%. ^1H NMR (400 MHz, $CDCl_3$): $\delta = 3.10$ (m, 12H; CH_2), 2.70 (t, 2H; CH_2), 2.55 (t, 2H; CH_2), 1.86 (q, 2H; CH_2), 1.63 (q, 2H; CH_2), 1.38 (s, 27H; $C(CH_3)_3$); MS (ESI): *m*/*z*: 501.2 $[M+H]^+$.

1-Dansylamidoethyl-1,4,8-tris(*tert*-butoxycarbonyl)-1,4,8,11-tetraazacyclotetradecane (5): Compound **4** (0.5 g, 1 mmol) was dissolved in dry

0947-6539/02/0821-4970 $ 20.00+.50/0 *Chem. Eur. J.* **2002**, *8*, No. 21

acetonitrile (30 mL), and a solution of dansylaziridine (276 mg, 0.9 mmol) in dry acetonitrile (15 mL) was added dropwise. The reaction mixture was refluxed overnight under a dinitrogen atmosphere. Solvent was removed with a rotary evaporator and the crude yellow oil was purified by liquid chromatography (silica gel, hexane/ethyl acetate 1:1, $R_f = 0.25$); yield 54.7%. MS (ESI): m/z: 774.1 $[M+H]^+$; elemental analysis calcd (%) for $C_{39}H_{64}N_6SO_8$ (773.0): C 60.28, H 8.30, N 10.82; found: C 60.13, H 8.49, N 11.10.

1-Dansylamidoethyl-1,4,8,11-tetraazacyclo-tetradecane (3; LH): Compound **5** (0.42 g, 0.62 mmol) was dissolved in trifluoroacetic acid (30 mL) and the solution was stirred at room temperature under a dinitrogen athmosphere for 24 h. Solvent was removed with a rotary evaporator and the crude product was dissolved in aqueous HCl 10% (30 mL) and extracted with dichloromethane (2×25 mL). Water solution was then adjusted to pH 10 with aqueous 3M NaOH and extracted with dichloromethane (3×25 mL); the combined organic layers were dried over $NaSO_4$ and the solvent evaporated in vacuo, giving compound **3** (232.1 mg, 78.6%). ^{1}H NMR (400 MHz, $CDCl_3$): $\delta = 8.48$ (d, 1H; ArH), 8.46 (d, 2H; ArH) 8.21 (d, 1H; ArH), 7.50 (m, 2H; ArH), 7.15 (d, 1H; ArH), 3.02 (t, 2H; CH_2), 2.86 (s, 6H; CH_3), 2.83 (t, 2H; CH_2), 2.74–2.78 (m, 6H; CH_2), 2.69 (t, 2H; CH_2), 2.61 (t, 2H; CH_2), 2.47–2.51 (m, 4H; CH_2), 1.73 (m, 2H; CH_2), 1.67 (m, 2H; CH_2); MS (ESI): m/z: 477.4 $[M+H]^+$.

$[Ni^{II}(LH_{-1})]ClO_4$: Ligand **3** (0.128 mmol, 61 mg) was dissolved in ethanol/water 4:1 (1 mL), and the solution was adjusted to pH 7. A solution of 0.13M nickel(II) perchlorate in ethanol (1 mL, 1 equiv) was added and the mixture heated at 50°C for 30 min. The complex precipitated as a blue powder, which was collected by filtration (54.6 mg, 67.3%). MS (ESI): m/z: 534.5 $[M-ClO_4]^+$; elemental analysis calcd (%) for $C_{24}H_{39}ClN_6O_6SNi$ (633.8): C 45.48, H 6.20, N 13.26; found: C 45.13, H 6.12, N 13.33. Diffusion of diethyl ether into the mother liquor gave crystals suitable for X-ray crystallography.

$[Ni^{II}(LH)](ClO_4)_2$: Complex salt $[Ni^{II}(LH_{-1})]ClO_4$ (0.08 mmol, 50 mg) was dissolved in ethanol/water 4:1 (2 mL) and aqueous 1M perchloric acid (about 0.1 mL) was added until the blue solution turned yellow. The complex salt precipitated as yellow-orange powder after volume reduction and was collected by filtration (34.2 mg, 58.2%). MS (ESI): m/z: 635.3 $[M-ClO_4]^+$; elemental analysis calcd (%) for $C_{24}H_{40}Cl_2N_6NiO_{10}S$ (734.3): C 39.26, H 5.49, N 11.45; found: C 39.54, H 5.62, N 11.25.

X-ray Crystallographic studies: Crystal data for complex $[Ni^{II}(LH_{-1})](ClO_4)\cdot(H_2O)$ are reported in Table 1 while selected bond lengths and angles are reported in Figure 3. Unit cell parameters and intensity data were obtained on a Bruker AXS CCD four-circle diffractometer at room temperature using graphite-monochromatized $Mo_{K\alpha}$ radiation ($\lambda = 0.71073$ Å). Parameters of CCD data collection and of subsequent structure refinement are also summarized in Table 1. The SMART system of programs was used for crystal lattice determination and X-ray data collection, SAINT+ for the data reduction including intensity integration, background and Lorentz polarization corrections. A semiempirical absorption correction based on the determination of transmission factors for equivalent reflections was applied using the program SADABS (SMART, SAINT+ and SADABS are all Bruker products). The structure was solved by direct methods using SIR-92[21] and refined by full-matrix least squares using SHELX-97.[22] Atomic scattering factors were taken from *International Tables for X-ray Crystallography*.[23] Diagrams of the molecular structure were produced by the ORTEP-3 program.[22] The final refinement was performed with anisotropic displacement parameters for all the non-hydrogen atoms; hydrogen atoms were inserted in the calculated positions and refined with isotropic displacement parameters proportional to those of the neighboring atoms. Hydrogen atoms of the water molecule were not located in the difference-Fourier maps and were then disregarded.

Crystallographic data (excluding structure factors) for the structure reported in this paper have been deposited with the Cambridge Crystallographic Data Centre as supplementary publication no. CCDC-184562. Copies of the data can be obtained free of charge on application to CCDC, 12 Union Road, Cambridge, CB2 1EZ, UK (fax: (+44) 1223-336-033; e-mail: deposit@ccdc.cam.ac.uk).

Table 1. Crystal data, data collection information and refinement details.[a]

formula	$NiN_6SC_{24}H_{41}O_7Cl$
F_w	651.8
crystal size [mm]	$0.50 \times 0.50 \times 0.20$
crystal system	orthorhombic
space group	*Pbca*
a [Å]	15.1145(30)
b [Å]	13.4135(27)
c [Å]	28.6592(57)
V [Å^3]	5810.3(2)
$F(000)$	2712
Z	8
ρ_{calcd} [g cm^{-3}]	1.479
μ [mm^{-1}]	0.884
T [K]	298(3)
total number of frames	1321 (size: 512×512 pixels)
detector-sample distance [cm]	5.000
scan type	ω
scan width [°]	0.3
scan time [sec]	10
θ_{max} [°]	25.51
index ranges	$-18 \le h \le 18$, $-16 \le k \le 16$, $-34 \le l \le 34$
reflns measured/unique	53610/5402 ($R_{int} = 0.036$)
refinement type	F^2
R_1[b]	0.0665
R_{all}	0.0747
wR_2	0.1751
GOF[c]	1.119
refined parameters	363
$(shift/e.s.d.)_{max}$	0.000
max, min $\Delta\rho$ [e × Å^{-3}]	0.897, −0.349

[a] Weighting scheme $w = 1/[\sigma^2(F_o^2)+(0.0874P)^2+7.997P]$ where $P = (F_o^2+2F_c^2)/3$. [b] $R_1 = \Sigma||F_o|-|F_c||/\Sigma|F_o|$ (calculated on 721 reflections with $I > 2\sigma_I$). [d] $GOF = S = [\Sigma[w(F_o^2 - F_c^2)^2]/(n-p)]^{0.5}$, where n is the number of reflections and p is the total number of parameters refined.

Acknowledgements

The financial support of the European Union (RTN Contract HPRN-CT-2000-00029) and the Italian Ministry of University and Research (PRIN 2001 Dispositivi Supramolecolari) is gratefully acknowledged. We are indebted to Dr. Eleonora Perani for assistance with mass spectra determination.

[1] a) V. Balzani, M. Gomez-Lopez, J. F. Stoddart, *Acc. Chem. Res.* **1998**, *31*, 405–414; b) J.-P. Sauvage, *Acc. Chem. Res.* **1998**, *31*, 405–414; c) V. Balzani, A. Credi, F. M. Raymo, J. F. Stoddart, *Angew. Chem.* **2000**, *112*, 3484–3530; *Angew. Chem. Int. Ed.* **2000**, *39*, 3348–3391; d) V. Amendola, L. Fabbrizzi, C. Mangano, P. Pallavicini, *Acc. Chem. Res.* **2001**, *34*, 488–493.

[2] a) G. Schill, *Catenanes, Rotaxanes and Knots*, Academic Press, New York, **1971**; b) Molecular Catenanes, Rotaxanes and Knots (Eds.: J.-P. Sauvage, C. O. Dietrich-Buchecker), Wiley-VCH, Wienheim, **1999**.

[3] a) R. A. Bissel, E. Cordova, A. E. Kaifer, J. F. Stoddart, *Nature* **1994**, *369*, 133–137.

[4] a) P. Gaviña, J.-P. Sauvage, *Tetrahedron Lett.* **1997**, *38*, 3521–3524; b) J.-P. Collin, P. Gaviña, J.-P. Sauvage, *New J. Chem.* **1997**, *21*, 525–528; c) N. Armaroli, V. Balzani, J.-P. Collin, P. Gaviña, J.-P. Sauvage, B. Ventura, *J. Am. Chem. Soc.* **1999**, *121*, 4397–4408.

[5] a) M. Asakawa, P. R. Ashton, V. Balzani, A. Credi, C. Hamers, G. Mattersteig, M. Montalti, A. N. Shipway, N. Spencer, J. F. Stoddart, M. S. Tolley, M. Venturi, *Angew. Chem.* **1998**, *110*, 357–361; *Angew. Chem. Int. Ed.* **1998**, *37*, 333–337; b) V. Balzani, A. Credi, S. J. Langford, F. M. Raymo, J. F. Stoddart, M. Venturi, *J. Am. Chem. Soc.* **2000**, *122*, 3542–3543; c) P. R. Ashton, R. Ballardini, V. Balzani, A. Credi, M. T. Gandolfi, S. Menzer, L. Perez-Garcia, L. Prodi, J. F.

Stoddart, M. Venturi, A. J. P. White, D. J. Williams, *J. Am. Chem. Soc.* **1995**, *117*, 11171 – 11197; d) A. Livoreil, C. O. Dietrich-Buchecker, J.-P. Sauvage, *J. Am. Chem. Soc.* **1994**, *116*, 9399 – 9400; e) F. Baumann, A. Livoreil, W. Kaim, J.-P. Sauvage, *Chem. Commun.* **1997**, 35 – 36.
[6] P. R. Ashton, R. Ballardini, V. Balzani, S. E. Boyd, A. Credi, M. T. Gandolfi, M. Gomez-Lopez, S. Iqbal, D. Philp, J. A. Preece, L. Prodi, H. G. Ricketts, J. F. Stoddart, M. S. Tolley, A. J. P. White, D. J. Williams, *Chem. Eur. J.* **1997**, *3*, 152 – 170.
[7] P. Pallavicini, A. Perotti, B. Seghi, L. Fabbrizzi, *J. Am. Chem. Soc.* **1987**, *109*, 5139 – 5144.
[8] E. J. Billo, *Inorg. Chem.* **1984**, *23*, 236 – 238.
[9] a) T. J. Lotz, T. A. Kaden, *J. Chem. Soc. Chem. Commun.* **1977**, 15 – 16; b) T. J. Lotz, T. A. Kaden, *Helv. Chim. Acta* **1978**, *61*, 1376 – 1387.
[10] L. Fabbrizzi, M. Licchelli, P. Pallavicini, L. Parodi, *Angew. Chem.* **1998**, *110*, 938 – 841; *Angew. Chem. Int. Ed.* **1998**, *37*, 800 – 802.
[11] a) T. Koike, E. Kimura, I. Nakamura, Y. Hashimoto, M. Shiro, *J. Am. Chem. Soc.* **1992**, *114*, 7338 – 7345; b) T. Koike, T. Watanabe, S. Aoki, E. Kimura, M. Shiro, *J. Am. Chem. Soc.* **1996**, *118*, 12696 – 12703; c) G. K. Walkup, B. Imperiali, *J. Am. Chem. Soc.* **1996**, *118*, 3053 – 3054.
[12] S. Brandes, C. Gros, F. Denat, P. Pullumbi, R. Guilard, *Bull. Soc. Chim. Fr.* **1996**, *133*, 65 – 73.
[13] L. Sabatini, L. Fabbrizzi, *Inorg. Chem.* **1979**, *18*, 438 – 444.
[14] a) L. Fabbrizzi, M. Licchelli, P. Pallavicini, A. Perotti, A. Taglietti, D. Sacchi, *Chem. Eur. J.* **1996**, *2*, 75 – 82; b) M. R. Wasielewski, G. L. Gaines III, M. P. O'Neil, M. P. Niemczyk, W. A. Svec in *Supramolecular Chemistry* (Eds.: V. Balzani, L. De Cola), Kluwer Academic Publishers, Dordrecht, **1992**, p. 202.
[15] G. L. Gaines III, M. P. O'Neil, W. A. Svec, M. P. Niemczyk, M. R. Wasielewski, *J. Am. Chem. Soc.* **1991**, *113*, 719 – 721.
[16] L. Fabbrizzi, M. Licchelli, P. Pallavicini, A. Perotti, A. Taglietti, D. Sacchi, *Chem. Eur. J.* **1996**, *2*, 75 – 82.
[17] E. K. Barefield, F. Wagner, A. W. Herlinger, A. R. Dahl, *Inorg. Synth.* **1975**, *16*, 220 – 225.
[18] G. Gran, *Analyst* **1952**, *77*, 661.
[19] P. Gans, A. Sabatini, A. Vacca, *Talanta* **1996**, *43*, 1739 – 1753.
[20] W. C. Wolsey, *J. Chem. Educ.* **1973**, *50*, A335 – A337.
[21] A. Altomare, G. Cascarano, C. Giacovazzo, A. Gualardi, *J. Appl. Crystallogr.* **1993**, *26*, 343 – 350.
[22] G. M. Sheldrick, *SHELX-97*, Programs for Crystal Structure Analysis, University of Göttingen, Germany, 1998.
[23] *International Tables for X-ray Crystallography*, *Vol. 4*, Kynoch, Birmingham, England **1974**, pp. 99 – 101 and 149 – 150.
[24] L. J. Farrugia, *J. Appl. Crystallogr.* **1997**, *30*, 565.

Received: May 3, 2002 [F4056]

  0947-6539/02/0821-4972 $ 20.00+.50/0